ELSEVIER

Journal of Alloys and Compounds 356–357 (2003) 598–602

Journal of ALLOYS AND COMPOUNDS

www.elsevier.com/locate/jallcom

Hydrogenation properties of nanocrystalline Mg- and Mg_2Ni-based compounds modified with platinum group metals (PGMs)

O. Gutfleisch[a,*], N. Schlorke-de Boer[a], N. Ismail[a], M. Herrich[a], A. Walton[b], J. Speight[b], I.R. Harris[b], A.S. Pratt[c], A. Züttel[d]

[a]*Leibniz Institut für Festkörper- und Werkstoffforschung, IFW Dresden, Institute of Metallic Materials, P.O. Box 270016, D-01171 Dresden, Germany*
[b]*Department of Metallurgy and Materials, University of Birmingham, Birmingham B15 2TT, UK*
[c]*Johnson Matthey Technology Centre, Sonning Common, Reading RG4 9NH, UK*
[d]*Physics Department, University of Fribourg, 1700 Fribourg, Switzerland*

Received 10 June 2002; accepted 25 October 2002

Abstract

Nanocrystalline Mg-based compounds are attractive hydrogen storage materials. Further improved sorption kinetics can be combined with the intrinsically high storage capacity when using alloy additions or catalysts. In this work, platinum group metals (PGMs) have been employed to surface modify Mg- or Mg_2Ni-based compounds. Nanocrystalline powders have been synthesised by high energy ball milling in hydrogen or argon atmospheres. The effects of co-milling time with the PGM, the use of pre-hydrided Mg for inert milling and blending with minor amounts of Ni are investigated. Gravimetric and thermal desorption studies combined with microstructural analysis using HRSEM and XRD demonstrate the usefulness of nanocrystallinity, thermodynamic destabilisation of the hydride and the catalytic properties of PGMs resulting in much reduced desorption temperatures. Reactively milled Mg_2Ni co-milled for 1 h with Ru shows an onset temperature of hydrogen desorption as low as 80 °C.

Keywords: Hydrogen storage; Nanostructured materials; Kinetics; Magnesium hydride; High energy ball milling; Catalyst

1. Introduction

Hydrogen is of great interest as an ideal and clean source of energy conversion in the future. As hydrogen storage materials, magnesium and magnesium-based alloys are attractive for application due to their high hydrogen storage capacities (up to 7.6 wt.% for Mg), low cost and convenient hydride heats of formation. However, practical application is limited as the magnesium-based alloys suffer from sluggish sorption kinetics in such a way that Mg hydride needs to be heated to more than 300 °C for several hours to obtain pertinent sorption kinetics [1,2]. Recently, progress in hydride technology was achieved when Mg-hydride was prepared in a nanocrystalline microstructure using high-energy ball milling [3–8]. Preparation of Mg or MgH_2 in a nanocrystalline form by this means increases the surface area as well as introducing numerous grain boundaries and defects which facilitate the hydrogen penetration [9]. The absorption kinetics was improved in such a way that the duration of hydrogen charging was reduced to only a few minutes at 300 °C. Nonetheless, this temperature is still too high for many applications. Thus, several attempts have been made to enhance the surface kinetics using various additives as catalysts. Mainly 3d transition metals have been introduced as effective surface modifiers for magnesium, but also to destabilise the respective hydride phases. Liang et al. reported that by adding 5 at.% of Ti, V, Mn, Fe or Ni to high energy ball-milled MgH_2, absorption could be performed at room temperature (1 MPa) and desorption took place at 235 °C (0.015 MPa) [9,10]. Previously, Pd, Ni and Fe additives have been used to improve the dissociation of hydrogen on Mg_2Ni, FeTi and $LaNi_5$ surfaces [11–13]. Hydrogenation properties of AB_5 materials were shown to be effectively improved by Ru [14]. Recently, Oelerich et al. [15,16] showed that metal oxide catalysts such as Cr_2O_3 or V_2O_5 with a content as low as 0.2 mol.%, enhances the absorption–desorption kinetics of Mg and Mg-based alloys.

*Corresponding author. Tel.: +49-351-4659-664; fax: +49-351-4659-781.
E-mail address: o.gutfleisch@ifw-dresden.de (O. Gutfleisch).

0925-8388/02/$ – see front matter
doi:10.1016/S0925-8388(02)01283-5

Other attempts were carried out by co-milling Mg with mixtures of additives (Zr+Ti, Zr+Mn) or lithium, all resulting in reduction of the hydrogen absorption temperature [3].

In this work, in an attempt to improve the hydrogen sorption kinetics, various platinum group metals (PGMs) and minor alloying additions have been employed to (1) modify the surface of Mg and Mg_2Ni alloys and (2) destabilise the respective hydride phases.

2. Experimental

Magnesium powder of mesh size 45 μm and purity 99.8% was used to prepare microcrystalline (mc) Mg-hydride in a vessel (PARR-reactor) under a hydrogen (purity 99.99%) pressure of 60 bars and at a temperature of 400 °C for 3 h. To obtain a nanocrystalline microstructure (nc), MgH_2 is then high energy ball milled in a Retsch-mill under an argon atmosphere for 80 h. Here, PGM catalysts (0.5 wt.%) of the types Ru, $PdOH_2O$, Pt and Pd black were added from the start of the milling. All catalysts have a purity of 99.9% (products of Johnson Matthey). The ball to powder ratio was 10:1. In a second series of powder preparation, Mg_2Ni pieces were crushed to a mesh size <100 μm and this microcrystalline (mc) powder was then hydrogen charged at 300 °C under a hydrogen pressure of 25 bars for 3 h. Other Mg_2Ni powder samples of <250-μm mesh size were reactively milled (RM) in a P6 planetary ball mill under a hydrogen atmosphere of 7 bars for 80 h to obtain nc-Mg_2NiH_4 powder. The ball to powder ratio was 13:1. Here, PGMs catalysts (1 wt.%) were added after the RM treatment and the powder preparation was concluded with 1 h of co-milling. Hydrogen thermal desorption analysis was performed in a dynamic vacuum using a heating rate of 10 K/min. All the milled powders were handled in a glove box under a purified Ar atmosphere of oxygen content <1 ppm. The hydrogen content was measured by hot extraction using a LECO 402 hydrogen analyser. The nanostructure after intensive milling was investigated by X-ray diffraction (XRD) using a Philips PW 1050 diffractometer and Co K_α radiation. The surface morphology and microstructure of MgH_2 and Mg_2Ni with different catalysts were investigated by means of field emission gun scanning electron microscopy (FEGSEM LEO 1530) equipped with EDX analysis. An Intelligent Gravimetric Analyser (IGA Hiden Analytical) was used to measure hydrogen sorption isotherms up to 15 bar and temperatures of 200 and 300 °C. Samples were typically 100 mg in size.

3. Results and discussion

The as-prepared Mg-hydride exhibited a hydrogen content of 7.5 wt.%. Fig. 1 reveals a fully crystalline diffraction pattern of the MgH_2 phase obtained after charging in the reactor (pattern (a)). After intensive milling in an inert atmosphere for 80 h, the peaks of the MgH_2 pattern are broadened indicating the formation of a nanocrystalline structure and some MgO minority phase (pattern (b)). The thermal desorption behaviours of different MgH_2 samples are represented in Fig. 2. As expected, nc-MgH_2 starts to desorb at lower temperatures than those of the mc-MgH_2 counterpart. The onset of the broad desorption peak of the nc-hydride is at about 220 °C (curve b) while a much sharper desorption peak of the mc-hydride occurs at 370 °C (curve a). As a fully crystalline hydride structure has a definite decomposition energy, hydrogen desorption takes place at a well defined peak temperature. On the other hand, the nanocrystalline structure is metastable and has a high volume fraction of grain boundaries and defects. Thus, it is possible that decomposition and desorption of hydrogen takes place over a range of temperatures, hence the broader desorption curve observed. Fig. 2 shows also the desorption curves of MgH_2 samples co-milled with

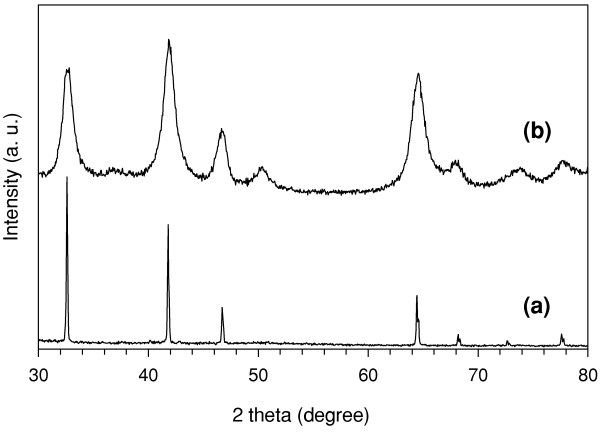

Fig. 1. X-ray diffraction patterns of (a) microcrystalline MgH_2 and (b) nanocrystalline MgH_2 after intensive milling for 80 h.

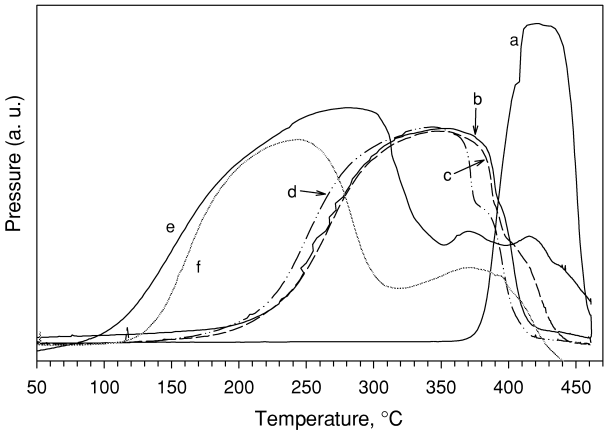

Fig. 2. Hydrogen desorption curves of (a) mc-MgH_2; (b) nc-MgH_2; nc-MgH_2 co-milled for 80 h with (c) 0.5 wt.% Pt black; (d) 0.5 wt.% $PdOH_2O$; (e) 0.5 wt.% $PdOH_2O$+5 at.% Ni; (f) 0.5 wt.% $PdOH_2O$+10 at.% Ni.

PGMs from the beginning. Powders with Pt black (curve c) and $PdOH_2O$ (curve d) show a similar desorption behaviour as nc-MgH_2. The hydrogen desorption temperature is reduced significantly to less than 140 °C when MgH_2 is co-milled with 0.5 wt.% $PdOH_2O$ and 5 at.% (curve e) or 10 at.% (curve f) Ni.

The apparent activation energy of the hydride decomposition, *E*, was calculated using the Kissinger method [17] for different hydrogen desorption heating rates of 2, 5, 10 and 20 K/min. The *E* values of nc-MgH_2 and nc-MgH_2+0.5 wt.% $PdOH_2O$ co-milled for 80 h are 59 and 64 kJ/mol H_2, respectively, i.e. no significant difference is found. A lower hydrogen decomposition energy of 47 kJ/mol H_2 was estimated for nc-MgH_2+0.5 wt.% $PdOH_2O$+10 at.% Ni. Co-milling with the catalyst (0.5 wt.%) from the start with nc-MgH_2 is kinetically not effective, which is attributed to the diffusion of the catalyst into the bulk of the particle during milling. Thus, the catalyst does not contribute to the surface modification. Consequently, no difference in the hydrogen decomposition temperature was observed. However, as expected, the addition of Ni thermodynamically destabilises the hydride leading to a lower hydrogen desorption temperature consistent with the lower hydrogen decomposition energy.

The desorption curves of Mg_2NiH_4 samples are shown in Fig. 3. The onset of the hydrogen desorption of the mc-hydride sample (<100 μm) takes place at 185 °C (curve a), while the reactively milled nc-Mg_2NiH_4 starts to desorb at 140 °C (curve b). Hydrogen desorption curves of nc-Mg_2NiH_4 co-milled with 1 wt.% PGM catalysts for 1 h at the end, are also shown in Fig. 3 (curves c, d and e). Hydrogen desorption of the sample with Pd black starts at about 120 °C. A further reduction of the hydrogen desorption temperature is obtained in a sample with $PdOH_2O$, where the desorption takes place at about 100 °C (curve d). An even lower onset temperature of hydrogen desorption of about 80 °C is found when using 1 wt.% Ru (curve e). Most of the hydrogen desorption curves exhibit more than one peak. The first peak is broad, ending at temperatures around 300 °C where almost all of the hydrogen is desorbed. This is followed by smaller and sharper peaks, which are attributed to the desorption from more stable hydride phases. Thus, in all cases co-milling with PGMs catalysts for 1 h at the end reduces very effectively the desorption temperature.

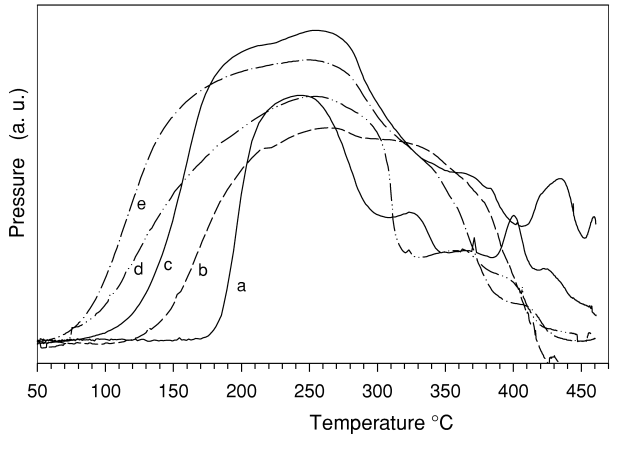

Fig. 3. Hydrogen desorption curves of (a) mc-Mg_2NiH_4; (b) nc-Mg_2NiH_4 (after RM); nc-Mg_2NiH_4 co-milled for 1 h with (c) 1 wt.% Pd black; (d) 1 wt.% $PdOH_2O$; (e) 1 wt.% Ru.

SEM images of reactively milled nc-Mg_2NiH_4, which was co-milled for 1 h at the end with 1 wt.% $PdOH_2O$ or Ru are shown in Fig. 4. The powder morphology is in both cases irregular and individual particles show a fine layered surface (left). The backscattered electron image shows that the $PdOH_2O$ catalyst, possibly reduced to Pd-metal, is covering the surface of the individual particles as shown in Fig. 4a (right) which can be attributed to the ductility of Pd. On the other hand, it appears that individual Ru particles of different sizes are homogeneously distributed on the particle surface (Fig. 4b (right)). This behaviour is consistent with the less ductile nature of Ru. It is possible therefore, that $PdOH_2O$ could have a dual role, combining a catalytic effect with oxidation protection of the hydride. It is not essential for effective catalysts to cover the whole surface and a homogeneous distribution of the catalyst particles is sufficient as this can lead to 'hydrogen spillover' effects [18].

Fig. 5 shows the IGA hydrogen absorption isotherms of nc-Mg_2Ni co-milled at the end with 1 wt.% $PdOH_2O$ (a) and Ru (b). Comparing the two diagrams, at 200 °C it is evident that saturation is reached at 4 bars in the case of $PdOH_2O$ and at 5 bars in the case of Ru. However, the maximum hydrogen content is 3.4 wt.% in the case of the sample containing Ru and only 2.8 wt.% in the case of the corresponding sample containing $PdOH_2O$. This fall-off in hydrogen capacity in the latter sample could be due to the relatively thick layer of Pd surrounding the particles as shown in Fig. 4a. Similar saturation values are attained at 300 °C but at higher pressures, 11 and 7 bar, for the $PdOH_2O$ and Ru containing samples, respectively.

4. Conclusions

Co-milling the nanocrystalline hydride with PGM catalysts for long durations results in diffusion of the catalysts into the bulk and consequently destroys its effectiveness at the surface. However, co-milling for short times, e.g. 1 h, leads to either a complete coating of the surface of individual particles as observed for $PdOH_2O$ or a homogeneous but discontinuous distribution on the surface as in the case of Ru, which allow the additives to act as hydrogen dissociation catalysts. Additionally, in the case of $PdOH_2O$ additions, the coating of Mg- or Mg_2Ni-type hydrides with the PGM catalyst could protect the surface from oxidation which can be considered to be an advantage for practical applications. The $PdOH_2O$ containing compound has a higher catalytic efficiency than Pd

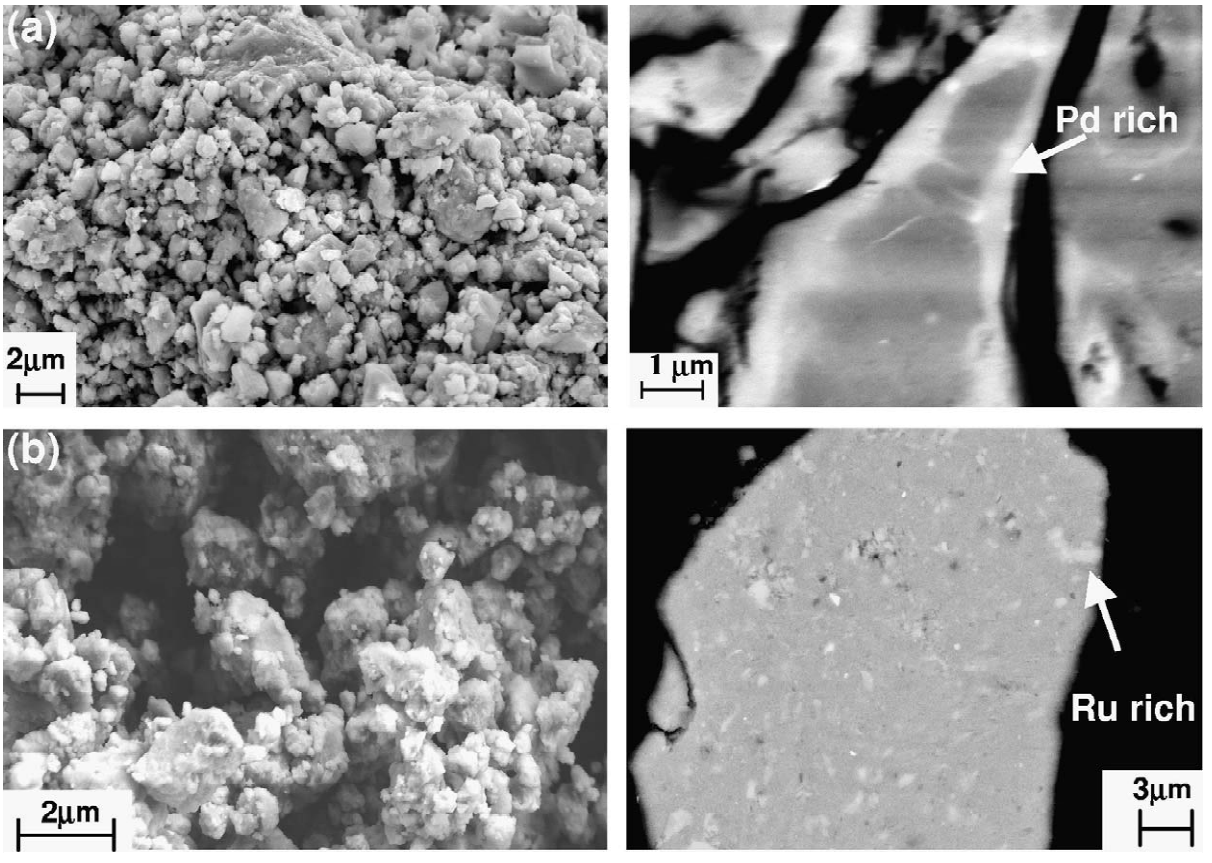

Fig. 4. SEM images in the secondary (left) and backscattered contrasts (right) of (a) nc-Mg_2NiH_4 co-milled for 1 h with 1 wt.% $PdOH_2O$ and (b) nc-Mg_2NiH_4 co-milled for 1 h with 1 wt.% Ru.

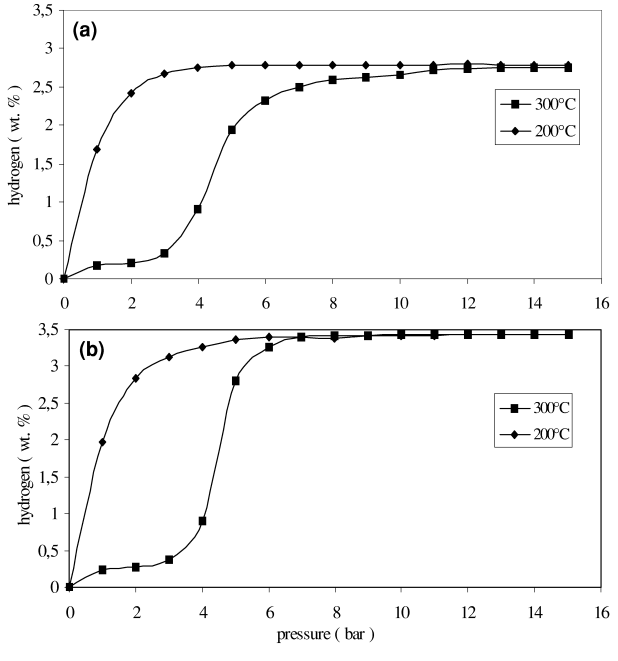

Fig. 5. IGA absorption isotherms at 200 and 300 °C of nc-Mg_2Ni co-milled for 1 h with 1 wt.% $PdOH_2O$ (a) and Ru (b).

black. By far the most effective catalyst, however, is Ru yielding also a higher absorption capacity for Mg_2Ni of 3.5 wt.% hydrogen. As expected, the addition of 3d elements such as Ni thermodynamically destabilises the Mg-hydrides. Hence, hydrogen desorption is faster.

Acknowledgements

The financial support by the EU project FUCHSIA (Part of the 5th Framework Energy Program) is gratefully acknowledged.

References

[1] L. Belkbir, E. Joly, N. Gerard, Int. J. Hydrogen Energy 6 (1981) 285.
[2] B. Bogdanovic, K. Bohmhammel, B. Christ, A. Reiser, K. Schlichte, R. Vehlen, U. Wolf, J. Alloys Comp. 282 (1999) 84.
[3] A. Zaluska, L. Zaluski, J.O. Ström-Olsen, J. Alloys Comp. 288 (1999) 217.
[4] A. Zaluska, L. Zaluski, J.O. Ström-Olsen, J. Alloys Comp. 289 (1999) 197.
[5] J. Huot, G. Liang, S. Boily, A.V. Neste, R. Schulz, J. Alloys Comp. 293–295 (1999) 495.

[6] S. Orimo, H. Fujii, K. Ikeda, Acta Mater. 45 (1996) 331.
[7] J.-L. Bobet, B. Chevalier, M.Y. Song, B. Darriet, J. Etourneau, J. Alloys Comp. 336 (2002) 292.
[8] J.-L. Bobet, E. Akiba, Y. Nakamura, B. Darriet, Int. J. Hydrogen Energy 25 (2000) 987.
[9] G. Liang, J. Huot, S. Boily, A. Van Neste, R. Schulz, J. Alloys Comp. 291 (1999) 295.
[10] J. Huot, J.F. Pelletier, G. Liang, M. Sutton, R. Schulz, J. Alloys Comp. 330–332 (2002) 727.
[11] E. Fromm, H. Uchida, J. Less-Common Met. 131 (1987) 1.
[12] H. Uchida, H.-G. Wulz, E. Fromm, J. Less-Common Met. 172 (1991) 1076.
[13] A. Zaluski, L. Zaluska, P. Tessier, J.O. Ström-Olsen, R. Schulz, J. Alloys Comp. 271 (1995) 295.
[14] D.B. Wiley, I.R. Harris, A.S. Pratt, J. Alloys Comp. 293–295 (1999) 613.
[15] W. Oelerich, T. Klassen, R. Bormann, J. Alloys Comp. 315 (2001) 237.
[16] W. Oelerich, T. Klassen, R. Bormann, J. Alloys Comp. 322 (2001) L5.
[17] H.E. Kissinger, J. Res. Natl. Bur. Stand. 57 (1956) 217.
[18] W.C. Connor (Ed.), Proc. 1st Int. Conf. Spillover, Lyon, France, 1983, University of Claude Bernard, Lyon-Vieurbanne, 1984, p. 71, Volume of Discussion.